



# Using equiluminance settings to estimate the cardinal chromatic directions for individuals

ALEX J. RICHARDSON,<sup>1,\*</sup> KASSANDRA R. LEE,<sup>2</sup>  MICHAEL A. CROGNALE,<sup>1,2</sup> AND MICHAEL A. WEBSTER<sup>1,2</sup> 

<sup>1</sup>Cognitive and Brain Sciences, Department of Psychology, University of Nevada, Reno, Reno, Nevada, 89557, USA

<sup>2</sup>Integrative Neuroscience, University of Nevada, Reno, Reno, Nevada 89557, USA

\*mwebster@unr.edu

Received 3 November 2022; revised 17 January 2023; accepted 18 January 2023; posted 23 January 2023; published 23 February 2023

Color information is processed by the retina and lateral geniculate along principal dimensions known as the cardinal directions of color space. Normal differences in spectral sensitivity can impact the stimulus directions that isolate these axes for individual observers and can arise from variation in lens and macular pigment density, photopigment opsins, photoreceptor optical density, and relative cone numbers. Some of these factors that influence the chromatic cardinal axes also impact luminance sensitivity. We modeled and empirically tested how well tilts on the individual's equiluminant plane are correlated with rotations in the directions of their cardinal chromatic axes. Our results show that, especially for the SvsLM axis, the chromatic axes can be partially predicted by luminance settings, providing a potential procedure for efficiently characterizing the cardinal chromatic axes for observers. © 2023 Optica Publishing Group

<https://doi.org/10.1364/JOSAA.480055>

## 1. INTRODUCTION

In the retina and lateral geniculate nucleus, chromatic information is primarily encoded within mechanisms thought to represent two opponent dimensions of color [1]. These dimensions correspond to two physiologically distinct channels that differentiate the cone signals of the long-wavelength-sensitive ( $L$ ) and medium-wavelength-sensitive ( $M$ ) cones (LvsM) and difference the signals of the short-wavelength-sensitive ( $S$ ) cones versus the  $L$  and  $M$  cones (SvsLM). These dimensions, which have been termed the “cardinal axes” of color space [2], are now very widely used to specify and examine the properties of human color vision, and form the axes of the standard physiologically defined color spaces of MacLeod and Boynton [3] and Derrington *et al.* [4].

Despite the importance of these axes, few studies attempt to specify the stimulus variations that isolate them for individual observers and instead assume a “standard observer” based on the average of a restricted number of individuals. This practice suffices for many applications of color science but is undesirable when precise or observer-specific calibrations are required and stands in stark contrast to the standard procedures for calibrating for individual differences in luminance sensitivity [5].

Normal variation in spectral sensitivity can produce individual differences in many aspects of color vision including color matching. These spectral sensitivity variations arise from many known physiological factors including individual differences

in the relative numbers of the different cone types, the spectral peaks, optical density of cone photopigments, as well as differences in macular pigment and lens pigment density [6,7]. Individual variations in these factors can also create challenges for accurate color reproduction within and across devices (e.g., monitors, projectors, printers, etc.). Specifically, problems could arise if colors produced by one device are not accurately reproduced for a different device across observers. For example, modern displays have progressed to feature high dynamic range and wide gamut lighting made possible by utilizing LEDs, OLEDs, and lasers. These technologies use primaries with narrowband spectra, allowing for a larger gamut containing a greater amount of potential colors, but could also increase errors in precise color reproduction due to the individual variation across observers [8].

Quantifying individual differences in color vision has been approached in a number of ways. One of these is to directly measure the color matching functions or stimuli of interest (e.g., cone isolating axes) for the observer. A second approach would be to directly measure the sources of variation, for example, determining the density of the lens or macular pigments, and then using these to indirectly predict the color matches for the observer. However, both approaches are laborious and often require specialized equipment. Here, we explore a third approach, based on direct measurements of luminance sensitivity and applying these to indirectly estimate aspects of chromatic sensitivity. In a previous study [9], we showed that many of the factors affecting luminance sensitivity (e.g., lens and macular pigment density) also impact spectral sensitivity, and thus

measurements of luminance sensitivity could be used to predict some of the variations in color matching. Here, we extend this logic to specifically examine how well one can estimate an observers' cardinal chromatic axes from their luminance settings. We also extend our previous work by not only modeling, but also empirically testing these predictions.

An advantage of this approach is that equiluminance settings for individual observers can be and are commonly assessed by a variety of techniques that provide rapid and accurate estimates. These standard techniques include heterochromatic flicker photometry [10,11] and minimum motion [12]. In contrast, as we noted, determining the cardinal chromatic axes is rarely undertaken, and while a number of techniques have been developed to assess individual differences in these axes, they are again time consuming and involve specialized procedures, such as the use of auxiliary adapting fields [13–15,15,16]. Despite this, spectral sensitivity variations can lead to significant changes in the stimuli that isolate the cardinal chromatic axes. These effects were explored in detail by Smith and Pokorny [17], who modeled the effects of different sources of variability on the luminance and chromatic axes, and how these variations might impact tasks, such as color discrimination. Our paper closely follows from theirs but is specifically focused on assessing how closely yoked the changes in the chromatic axes and luminance axis are. A strong correlation would indicate that the chromatic axes could be predicted from the luminance measures alone, and thus could allow better specification of an individual's color vision without additional equipment or measurements.

To address these questions, we first modeled the direction of an individual's cardinal axes predicted by normal variations in optical or photopigment variations and then compared how these factors jointly affect luminance sensitivity and the chromatic axes. We then sought to validate the model with psychophysical measures of the stimulus directions that isolate an individual's cardinal opponent axes. Results from the model indicate that routinely measured differences in luminance can provide partial (but not complete) information about the cone-opponent directions of an individual observer, although in practice the predicted variations were limited to the SvsLM axis. This suggests that exploiting luminance measurements to predict chromatic sensitivity has the potential of leading to better specification of the color spaces for an individual observer and comes "for free" in experiments that are already employing standard techniques for specifying luminance sensitivity.

## 2. METHODS

### A. Model

We modeled variations in spectral sensitivity (fundamentals) based on estimates of normal variability in the factors affecting the cone fundamentals. Methods for modeling the observers are similar to those used in previous studies [18–20]. We used Monte Carlo simulations to generate 1000 observers, each varying randomly over a range of  $\pm 2$  standard deviations in known factors that affect luminance and/or spectral sensitivity. These included: (1) lens pigment density (sd = 18.7% or 0.3 at 400 nm); (2) macular pigment density (sd = 36.5% or 0.13 at 458 nm); (3) independent variation in the spectral peak ( $\lambda_{\max}$ ) for each cone (sd = 2.0, 1.5, and 1.3 nm for  $L$ ,  $M$ , or  $S$  cones,

respectively); (4) independent variation in the optical density of the cone pigments (sd = 0.09 for  $L$  and  $M$ , and 0.074 for  $S$ ); and (5) independent variation in the  $LM$  cone ratios (logarithm change in the  $LM$  ratio, sd = 0.3). With the exception of  $LM$  cone ratios, the values for the standard deviations of the factors were based on Asano *et al.* [7]. The standard deviation of the cone ratios was assumed to be a fourfold change in the ratio based on Carroll *et al.* [21]. Each simulated observer was constructed by: (1) removing the assumed lens and macular filtering from the Stockman and Sharpe fundamentals; (2) shifting the absorption spectrum along the wavenumber axis to the chosen  $\lambda_{\max}$ ; (3) adjusting the optical density independently for each cone assuming an initial density of 0.35; and finally (4) screening by the random values for the lens and macular pigment density [22].

Once an observer was created, we calculated the luminance match, expressed as the angle of tilt of the equiluminant plane in the Derrington–Krauskopf–Lennie color space [4], relative to the standard observer plane. This space is not standardized, and the degree of tilt depends on the scaling assumed for the LvsM and SvsLM axes. For our analyses, we used the following scaling:

$$LvsM = 2754 * (l_{mb} - 0.6568),$$

$$SvsLM = 4099 * (s_{mb} - 0.01825),$$

$$LUM = 100 * LUM_{\text{test}}/LUM_{\text{ref}}$$

where  $l_{mb}$  and  $s_{mb}$  are the MacLeod–Boynton coordinates from which the coordinates of the nominal white point (corresponding to illuminant  $C$ ) are subtracted, and the values are then scaled by factors chosen so that the LvsM and SvsLM units roughly correspond to multiples of detection threshold [3,16]. For the current space, an azimuth of 0 deg corresponds to the  $+L$  direction in the LvsM axis, and 90 deg in azimuth corresponds to the  $+S$  direction in the SvsLM axis. An elevation of zero degrees corresponds to the nominal equiluminant plane, and an elevation of 90 deg is achromatic/white (CIE 1931 chromaticity of  $x = 0.31$ ;  $y = 0.316$ ). The luminance was scaled to correspond to 100 times the Weber contrast of the stimulus, again so that changes in luminance or chromaticity were roughly equated for multiples of threshold. The calculations estimated the tilt of the equiluminant plane and the corresponding rotations on the LvsM and SvsLM axes within the plane in terms of these scaled units for each observer. Note that for both the modeling and the psychophysics, the chromatic stimuli were varied on the plane of the standard observer and not for the plane adjusted for the luminance sensitivity of the individual.

### B. Psychophysics

We implemented two psychophysical experiments to empirically determine the tilt of the equiluminant plane and the location of the opponent axes for a set of observers. A minimum motion paradigm [12] was used for determining individual equiluminant settings/tilt of the equiluminant plane. Participants performed a 2AFC task to judge whether a grating appeared to drift either upward or downward, with the luminance difference within the chromatic grating varied in

a staircase. The equiluminance balance was determined by averaging the last 10 of 13 reversals of two interleaved staircases. The stimuli had a nominal mean photometric luminance of  $20 \text{ cd/m}^2$  and subtended  $2 \text{ deg}$  at a viewing distance of  $114 \text{ cm}$ . The patterns were  $0.5 \text{ c/deg}$  horizontal square-wave gratings and reversed in spatial and temporal quadrature at  $2.5 \text{ Hz}$ . Settings were made for chromatic gratings defined by two chromaticities that were  $\pm 80$  contrast units along the nominal LvsM or SvsLM axes. The Michelson contrast of the achromatic grating was  $10\%$ . Two to four measurements were made for each opponent axis.

A contrast-matching paradigm with selective chromatic adaptation was used to define the cardinal directions. This method is based on the procedure described in Webster *et al.* [16]. The stimulus appeared as two ( $1 \times 2$ )-deg adjacent rectangles (one top and one bottom) delimited from the background by solid black borders. Chromatic adaptation was implemented using a THOUSLITE LEDCube illuminant falling on a spectrally flat background, producing adaptation to short (peak  $\sim 425 \text{ nm}$ ) or long (peak  $\sim 635 \text{ nm}$ ) wavelength LEDs to reduce the sensitivity of the *S* cones or the *L* and *M* cones, respectively. Under these conditions, perceived contrast should therefore depend primarily on the cones under weaker adaptation. For example, in the presence of the shortwave adapting field, the *S* cones are more strongly adapted, and thus stimulus contrasts should mainly reflect the activity of the *L* and *M* cones. The chromatic direction of the stimulus can then be varied to find the point at which the perceived contrast is lowest, and this should correspond to the axis that minimizes the differences in the *L* and *M* cone signals. For this task, the choice of the adapting background is not critical since, for example, the isolation of the *S* axis depends primarily only on the change in *S*-cone sensitivity. Moreover, Webster and Mollon [15] showed that the *LM* and *S* axes empirically defined by this technique are also orthogonal with respect to a separate task based on contrast adaptation, suggesting the chromatic adaptation technique is successful in isolating the correct axes. In addition, other work has shown this technique agrees with other paradigms for isolating the tritanopic axis, such as transient tritanopia and minimal border [17]. To better estimate the threshold maxima, we used a comparison task as in Ref. [16] where stimuli defined by two different chromatic angles were presented at the same chromatic contrast, and the observer judged which had a higher perceived contrast. The null should then occur when the pair of directions straddle the SvsLM axis so that their perceived contrast is equal. The angles of the stimulus pair were varied within the nominal equiluminant plane and not corrected for the individual's luminance (since the luminance sensitivity is strongly affected by the chromatic adapting background and because the isolation is at the level of the cone responses).

Ten volunteers (seven male and three female) aged 24–65 yr participated as observers. All reported normal or corrected-to-normal acuity and no other inclusion/exclusion criteria were employed. The project was approved by the Institutional Review Board of The University of Nevada, Reno, and written informed consent was obtained from each participant. Observers were adapted to either the short or the long wavelengths while viewing a stimulus monitor through a beam splitter such that a uniform chromatic field was superimposed

over the view of the monitor. For the long-wavelength (red) adaptation, the chromaticity coordinates were  $x = 0.69$ ,  $y = 0.30$  with a luminance  $53 \text{ cd/m}^2$ . For the short (blue) wavelength adaptation, the chromaticity coordinates were  $x = 0.16$  and  $y = 0.04$  with a luminance of  $18 \text{ cd/m}^2$ . The participants viewed the pair of rectangular patches presented simultaneously above and below a fixation cross. The colors of the patches were nominally equiluminant and had a contrast of 80 units. They were separated by  $10 \text{ deg}$  in chromatic angle and were varied during the experiment to “straddle” the opponent axis being tested. The participants judged which of the two stimuli appeared higher in contrast. The mean color of the patches was then rotated in a staircase while maintaining the  $10$ -deg separation until the pair of colors appeared to be the same contrast. The individual's opponent axes were taken as the mean hue angle of the two comparison stimuli at the point of perceived equal or matching contrast, determined by the average of the past 10 of 13 reversals of the staircase. Observers repeated the task with both foveal and near-peripheral ( $4 \text{ deg}$  right and left) fixation with two to four settings made for each condition. Results reported are based on the mean settings for each observer and condition.

### 3. RESULTS

As noted, variations in luminance and spectral sensitivity arise from many factors. The effects of variations in each of the individual factors on the tilts versus rotations of the cardinal axes are illustrated in Fig. 1, which plots the range of variation in each cardinal axis predicted by a variation over  $\pm 2$  standard deviations in the value for each source of variation. Table 1 instead lists the magnitude of the angle changes for a  $\pm 1$  standard deviation change in each variable. For the table and all of the plots, a value of  $0 \text{ deg}$  corresponds to the nominal axes for a standard 2-deg observer. The ordinate gives the degrees of rotation within the chromatic plane away from the nominal axis for each cardinal axis (SvsLM or LvsM). The abscissa gives the amount of tilt away from the nominal equiluminant plane. In Fig. 1, only one factor was varied at a time, while the remaining were fixed at the standard observer. The figure shows that most of the predicted variations arise from the lens and macular pigment or the cone ratios with the variations in photopigment optical density or spectral peak contributing comparatively little to the effects.

The variations in lens and macular pigment density primarily affect the rotation of the SvsLM axis (top row). While both influence the relation between luminance and chromatic axes in similar ways, changes in the lens or macular pigment density do produce distinguishable changes in how the equiluminant plane itself tilts (i.e., the relation between *S* tilt and *LM* tilt—not plotted in the figures). These differences are shown in a previous paper where we show that these factors can be potentially estimated based on the differences in how they bias the equiluminant plane [9].

Changes in the *LM* cone ratios instead affect the direction of the LvsM axis (bottom row), while having no effect on the SvsLM axis. The reason for this influence is that the change in cone ratios alters the luminance ( $L + M$ ) sensitivity. The LvsM axis is also commonly referred to as the “constant-*S*” axis, along which signals in the *S* cones do not vary [2]. However, the actual

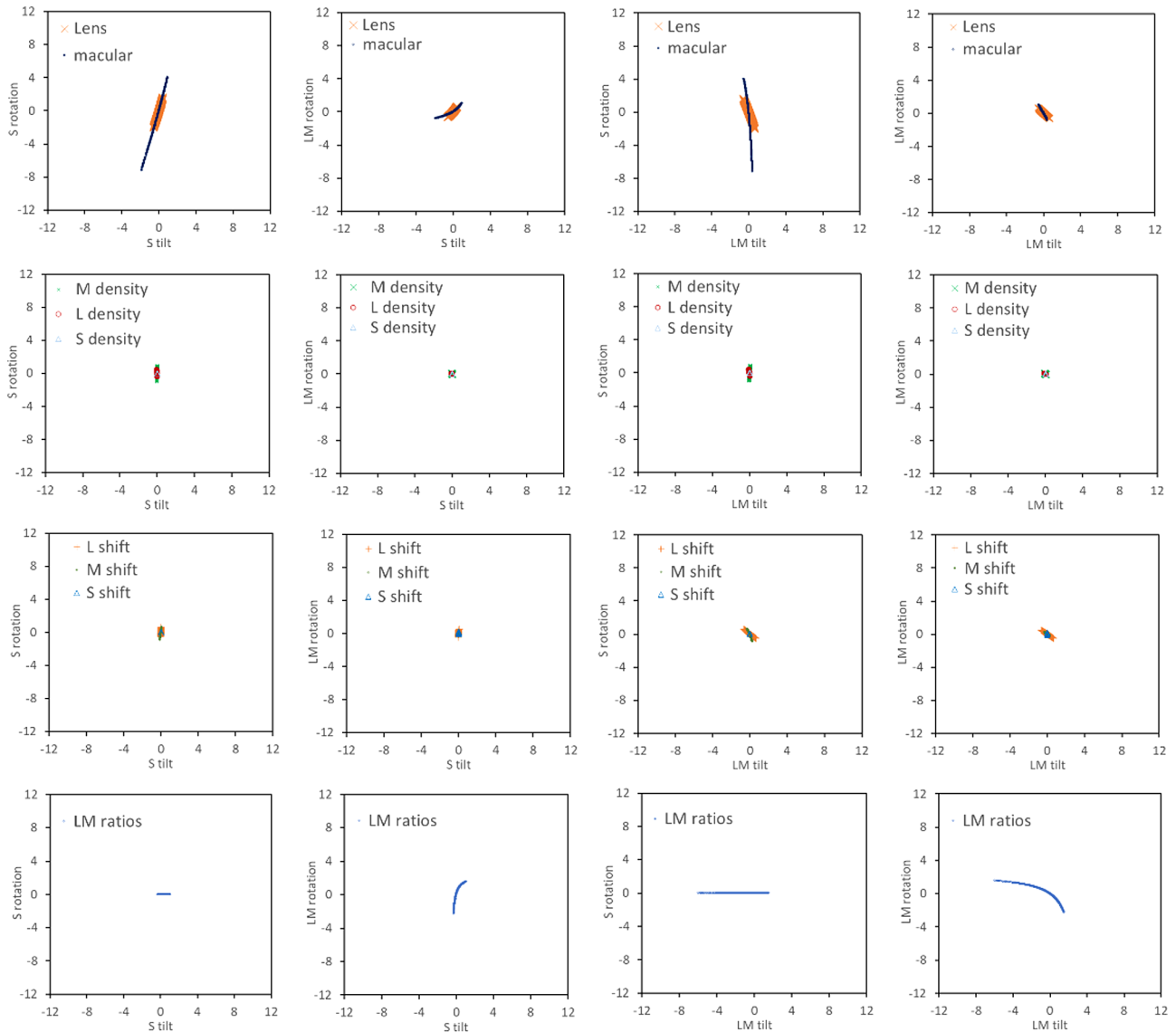


**Fig. 1.** Influence of each individual factor on the degrees of chromatic rotation ( $y$  axis) and tilt of the equiluminant plane ( $x$  axis). Top row shows effects of lens and macular pigment density variation. Second row shows effects of photopigment optical density changes for  $L$ ,  $M$ , and  $S$  cones. Third row shows impact of spectral peak shifts for  $L$ ,  $M$ , and  $S$  cones. Bottom row shows  $L/M$  cone ratios.

**Table 1. Magnitude of Angle Changes in Tilt or Rotation of the Cardinal Axes Predicted by a Change in ( $\pm$ ) One Standard Deviation in Each of the Individual Sources of Modeled Physiological Variation**

	S Tilt +1/ - 1 SD	LM Tilt +1/ - 1 SD	S Rotation +1/ - 1 SD	LM Rotation +1/ - 1 SD
$L$ optical density	-0.02/0.02	-0.03/0.03	0.2/-0.2	0.02/-0.03
$M$ optical density	-0.03/0.03	-0.04/0.03	-0.49/0.48	0.03/-0.03
$S$ optical density	0/0	0/0	0/0	0.01/-0.01
$L$ peak shift	-0.03/0.03	-0.33/0.34	0.31/-0.27	0.25/-0.25
$M$ peak shift	0.02/-0.02	0.16/0.15	0.34/-0.41	0.12/-0.11
$S$ peak shift	0/0	0/0	0/0	0.07/-0.06
Macular pigment	0.5/-0.74	-0.35/0.36	2.33/-3.12	0.48/-0.42
Lens density	0.17/-0.22	-0.35/0.37	0.89/-0.99	0.34/-0.27
$L/M$ ratios	0/0	-2.07/1.04	0/0	0.94/-1.15
All factors	0.77/-0.8	-3.97/1.98	3.23/-5.08	2.38/-2.29

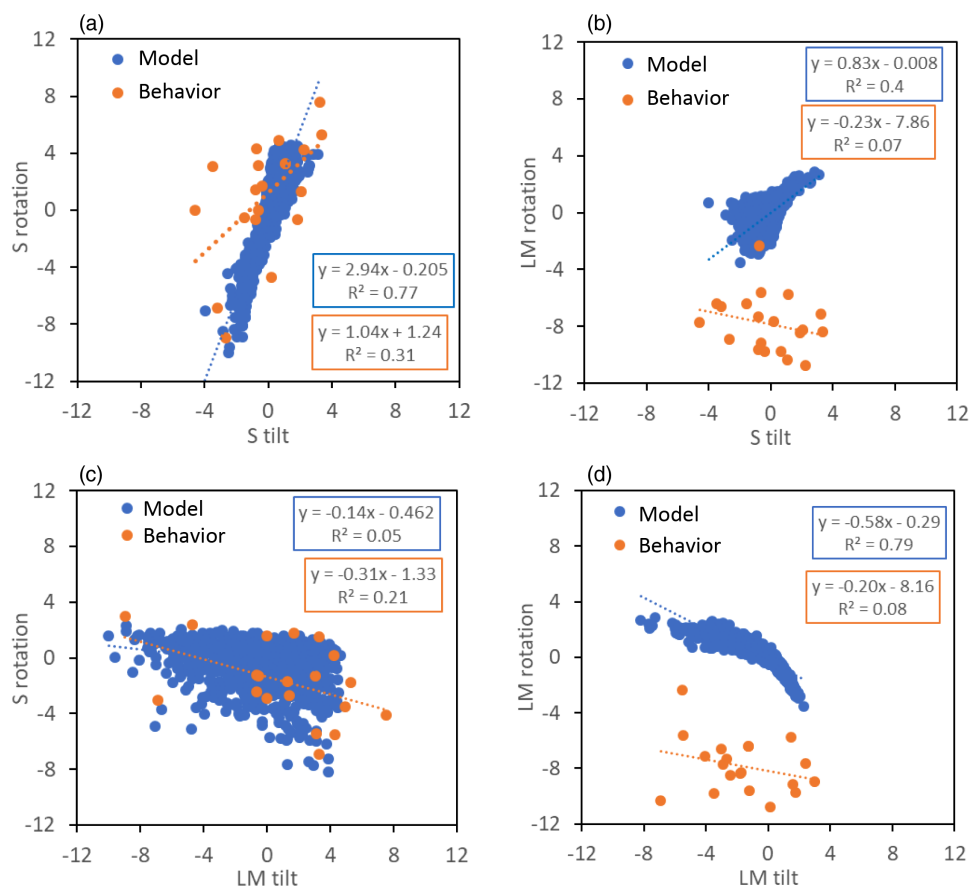
axis corresponds to “constant  $S/(L + M)$ ” since it is the axis for which the  $S$  signals remain constant at constant luminance. Since the cone ratios affect the value of  $L + M$  along the axis, the level of  $S$ -cone activity must also change to keep  $S/(L + M)$  constant. (This is also the case within the equiluminant plane for the observer since this intensity adjustment also affects the  $S$  cone responses to the stimuli, and thus does not affect the ratio of  $S$  to  $L + M$ ). In contrast, changes in the cone ratios do not affect the SvsLM axis because this axis instead corresponds to the axis along which  $L/(L + M)$  is constant, and this equivalence holds regardless of the  $LM$  ratio and consequent change in luminance sensitivity. We consider further below the implication of nulling the  $S$  versus the  $S/(L + M)$  signals to define the LvsM axis.

In the remaining analyses, we consider the potential combined effects of random variations in all of the factors. Since the different factors affect the axes in different ways, the luminance tilts and chromatic rotations are less tightly coupled than for the individual factors (Fig. 1), but strong covariations are still predicted. These are shown in Fig. 2, which presents the results from both the modeled (simulated) and the empirically measured observers to show the relationship between the variations in luminance ( $x$  axis) and the cardinal chromatic axes ( $y$  axis). The magnitudes of luminance tilt and chromatic rotation in the

SvsLM axis are strongly correlated for the simulated observers ( $r = 0.88$ ). This correlation was weaker for the actual observer, although still evident (both fovea and periphery  $r = 0.56$ ,  $p = 0.06$ ; just fovea  $r = 0.69$ ,  $p < 0.001$ ) [Fig. 2(a)].

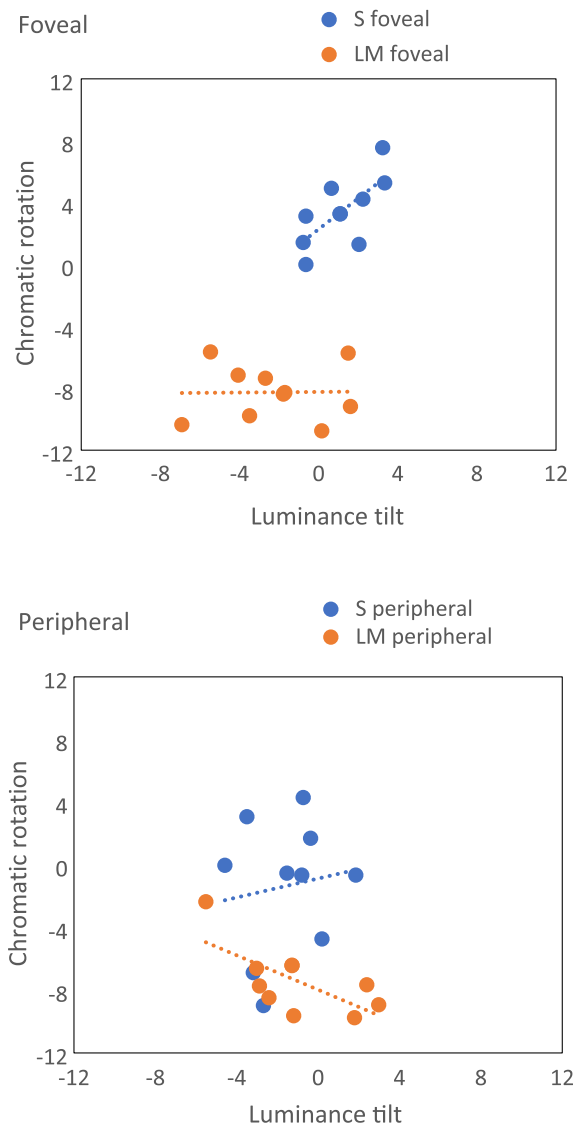
The predicted correlation for tilt and rotation in the LvsM axis was also strong for the simulations ( $r = 0.88$ ) but in this case was not significant for the measured observers ( $r = 0.28$ , NS) as shown in Fig. 2(d). The simulation data also predict that the  $S$  axis tilt should moderately correlate ( $r = 0.63$ ) with the chromatic rotation of the LvsM axis [Fig. 2(b)]. However, the behavioral data do not uphold this prediction and are instead poorly correlated ( $r = 0.26$ , NS). It can be seen in Fig. 2(c) that the simulated data show no meaningful correlation between the LvsM axis tilt and the SvsLM axis chromatic rotation ( $r = 0.22$ ), while the behavioral data show a slight moderate correlation ( $r = 0.46$  [ $p = 0.03$ ]). The empirically defined rotations of the LvsM axis were also consistently displaced from the standard observer. We are not sure of the basis for this, but a bias in the same direction was found in previous studies using different variants of the isolation method with different observers and hardware [16].

Figure 3 depicts the correlations for tilt and rotation for each axis in the behavioral data but for the separate foveal and peripheral conditions. Note that the axes in Fig. 3 represent



**Fig. 2.** Behavioral (orange) and modeled (blue) data showing correlation between degrees of chromatic rotation ( $y$  axis) and tilt of the equiluminant plane ( $x$  axis). (a) The magnitudes of luminance tilt and chromatic rotation in the SvsLM axis were strongly correlated for modeled observers, and weakly correlated for behavioral observers. (b) Modeled data predicted a weak correlation for  $S$  axis tilt with LvsM chromatic rotation. (c) Neither the modeled nor behavioral data showed correlations between LvsM axis tilt and the SvsLM chromatic rotation. (d) The correlation of tilt and rotation in the LvsM axis were strong for modeled observers but not significant for the measured observers.





**Fig. 3.** Correlations for tilt ( $x$  axis) and rotation ( $y$  axis) for each axis in the behavioral data. The top figure represents foveal conditions and shows a moderate correlation between luminance tilt and chromatic rotation for the SvsLM axis (blue plotted line). The LvsM axis showed no correlation (orange plotted line). In the peripheral condition (bottom), the LvsM axis showed a moderate correlation between tilt and rotation, while the SvsLM axis showed no correlation.

rotation along the chromatic axis ( $Y$ ) and tilt of the equiluminant plane ( $X$ ) for both LvsM (denoted as orange) and SvsLM (denoted as blue) axes. In the foveal condition, the SvsLM axis shows a moderate correlation ( $r = 0.69$ ,  $p < 0.05$ ), while the LvsM axis was uncorrelated ( $r = 0.04$ , NS). However, in the peripheral condition the LvsM axis was moderately correlated ( $r = 0.68$ ,  $p < 0.05$ ), while the SvsLM axis showed no correlation ( $r = 0.14$ , NS).

Note that the strength of the relationship between the tilt and the rotation may be underestimated from the linear correlation if the relationship is instead nonlinear [as evident in Fig. 2(d) for LvsM tilt versus rotation]. Moreover, for these linear correlations, we treated the tilt of the equiluminant plane as a separate parameter along each axis (i.e., as the tilt of SvsLM axis or the

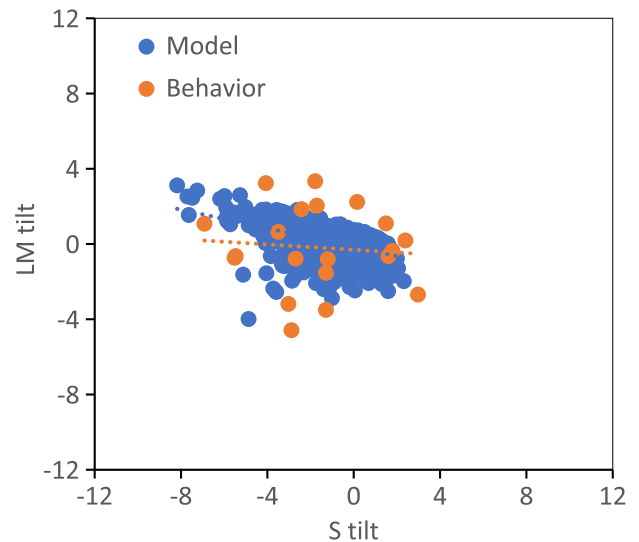


**Fig. 4.** Relationship between the luminance tilts of the SvsLM and LvsM axes from the equiluminant plane for both modeled (blue) and behavioral (orange) data. Both the model and the behavioral data show minimal correlations between tilts for either axis.

tilt of the LvsM axis). However, the tilt of the plane in color space requires two parameters (angles, here) in addition to the fixed white point for a unique determination. If the information provided by the two different axes is perfectly correlated, the information would be redundant, and only one tilt measure would be needed. A similar situation exists regarding the location of the chromatic axes. If the variation in the locations of the LvsM and SvsLM chromatic axes within the equiluminant plane are highly correlated, then the tilt of the equiluminant plane could predict the rotation of both axes. If, however, the LvsM and SvsLM parameters for the rotations and equiluminant tilts are independent of each other, then measuring the luminance tilts of both axes would provide additional information that

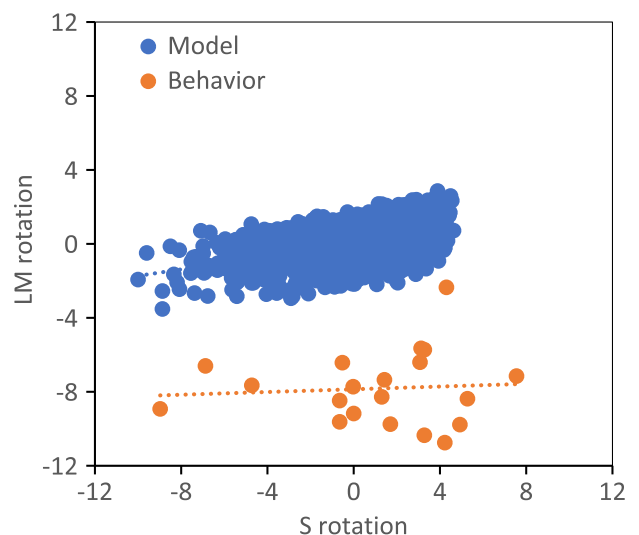


**Fig. 5.** Relationship between the chromatic rotations of the SvsLM and LvsM axes within the equiluminant plane for both modeled (blue) and behavioral (orange) data. For rotations of both cardinal axes, the model predicts a weak correlation. Behavioral data are uncorrelated for both axis rotations.

**Table 2. Correlation Matrices and Multiple Regression Results<sup>a</sup>**

$R^2$ Model				$R^2$ Behavior			
	SvsLM tilt	LvsM tilt	SvsLM rotation		SvsLM tilt	LvsM tilt	SvsLM rotation
LvsM tilt	0.25			LvsM tilt	0.008		
SvsLM rotation	0.77	0.05		SvsLM rotation	0.31	0.22	
LvsM rotation	0.4	0.77	0.2	LvsM rotation	0.065	0.081	0.005
Multiple regression (Model)				Multiple regression (Behavior)			
Adjusted $R^2$ (combined LvsM and SvsLM tilt)				Adjusted $R^2$ (combined LvsM and SvsLM tilt)			
SvsLM + LvsM tilt				SvsLM + LvsM tilt			
SvsLM rotation	0.83			SvsLM rotation	0.43		
LvsM rotation	0.83			LvsM rotation	0.062		

<sup>a</sup>Single parameter correlations from Figs. 2 and 4 (upper panels) compared to multiple-regression results using both LvsM and SvsLM axis tilts simultaneously to predict the rotation of each of the hue axes (lower panels). Left and right panels show model and behavioral data, respectively. Multiple regression model for predicting the SvsLM and LvsM axes compared to the predictions from tilts along a single axis, for simulations and behavioral results.

should better predict the rotations of each axis. Figures 4 and 5 assess these covariations by showing the predicted and observed relationships between the luminance tilts along either axis (Fig. 4) and the rotations within the chromatic plane (Fig. 5). For both the tilts and rotations, the model and behavioral measures suggest that the changes along the two axes are not tightly coupled.

Because the LvsM and SvsLM rotations and tilts are partially if not largely independent, then the combined information from the two axis tilts might better predict both rotations, and thus more completely specify an individual’s color space. Consequently, we combined the information from the two axis tilts to examine how much, if at all, the predictions of the hue axes were improved. Table 2 compares the single parameter correlations from Figs. 2 and 4 (upper panels) with the correlations using both LvsM and SvsLM axis tilts simultaneously to predict the rotation of each of the hue axes (lower panels). However, the multiple-regression results for the model appear to show only marginal improvement in the ability to predict the location of both the SvsLM ( $R^2 = 0.83$  versus  $0.77$  for  $S$  tilt alone) and the LvsM values ( $R^2 = 0.83$  versus  $0.77$  alone). The behavioral correlations are slightly stronger for the SvsLM rotation although the correlation for the LvsM axis remains very weak. Specifically, using the tilts along both axes to predict the rotations accounted for  $R^2 = 0.43$  and  $R^2 = 0.06$  percent of the variance in the rotations for the SvsLM and LvsM hue axes, respectively.

Overall, the results suggest that luminance tilts are partially predictive of the individual differences in the SvsLM axis, while failing to predict both the mean offset and uncorrelated changes along the LvsM axis. As noted, our model does not account for the mean differences. However, a potential basis for the discrepancy in the correlation is that the model is in fact correctly predicting the LvsM axis for different observers, while the behavioral settings are not. As discussed above, the modeled LvsM axis is defined by the axis of constant  $S/(L + M)$ . However the adapting procedure we used was instead designed to measure constant  $S$ -cone responses since it is based on strongly desensitizing the  $L$  and  $M$  cones, a procedure which should also strongly bias their relative sensitivity [23]. We therefore reran the model with all of the factors but so that the LvsM axis was based on constant- $S$  responses. This should remove most of the predicted variability in the LvsM rotations [since as Fig. 1 showed, these are primarily driven by the  $LM$  ratios, which affect  $S/(L + M)$  but not  $S$ ]. The results are shown in Fig. 6, and, in this case, the lack of a predicted correlation between the LvsM axis tilt and the rotation are now consistent with the observations. The implication is that the adapting paradigm we used is more effective for defining the SvsLM axis than the LvsM axis, at least, for participants with large biases in their  $LM$  cone ratios.

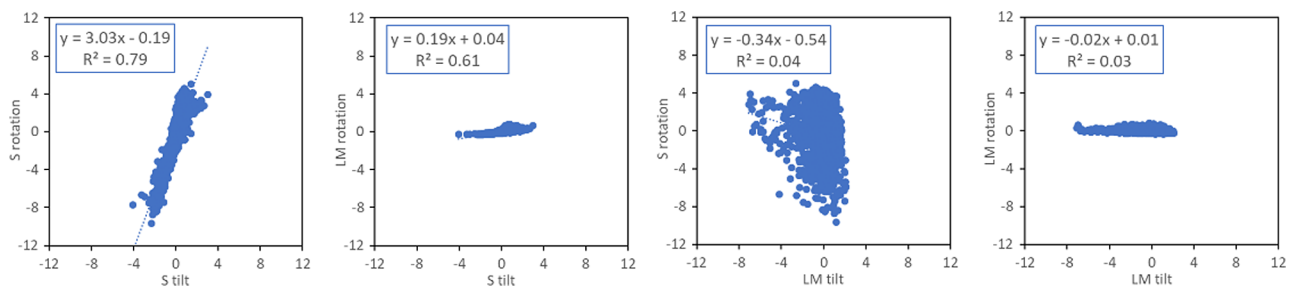


**Fig. 6.** Modeled relationship between the chromatic rotations of the SvsLM and LvsM axes within the equiluminant plane when the LvsM axis is based on constant  $S$ -cone activity rather than constant  $S/(L + M)$ . All factors were otherwise varied in the same way and over the same range ( $\pm 2$  SD) as in Fig. 2.

#### 4. DISCUSSION

As noted, there are large variations in normal color vision (Webster and MacLeod [6]; Asano *et al.* [7]), and these are important for specifying color for individual observers for different display devices (Smith and Pokorny [18]). With advances in display technology and applications, an increasingly important question is thus what the most accurate, practical, or efficient methods might be for calibrating displays for an individual. In a previous study, we showed that luminance settings can be used to partially predict and thus reduce errors in individual color matching functions because the luminance and spectral sensitivities are affected by common factors [9]. The rationale for that approach is that the factors affect luminance in different ways, and thus the values for different factors (e.g., lens or macular pigment density or cone ratios) can potentially be estimated from the pattern of tilt on the equiluminant plane. In turn, once these factors are estimated, they could be used to approximate the spectral sensitivity of the observer and thereby predict their color matches. Estimating three factors, such as both preretinal filters versus the cone ratios, would require three independent measurements of luminance sensitivity, which would instead be difficult to disentangle from only the two axes of tilt considered here or in conventional luminance measures [24]. While not articulated in our previous analysis, sufficient measures could, for example, be achieved for a single three-primary display by assessing the pattern of luminance tilt in both the fovea and the periphery (to separately estimate the macular pigment density).

Here we have extended this analysis to show that equiluminance settings can also lead to specific improvements in the specification of the cardinal chromatic axes defining color coding—and directly from the degree and pattern of the luminance tilt without the intervening step of modeling the observer's spectral sensitivity. While improvements to the technique and algorithm itself could lead to more accurate predictions, our goal was to show, in principle, that significant improvement over the standard observer (which is commonly assumed for the cardinal axes) is already potentially available to any study that is already correcting for an individual's equiluminant settings, a procedure that has itself become commonplace. The present results suggest that the SvsLM axis can be more accurately characterized for an individual simply from the observer's luminance sensitivity. While a number of techniques have been described for empirically specifying the cardinal axes [15], our method again has the potential to improve the estimate of the SvsLM and LvsM lines without requiring a separate procedure or auxiliary equipment, and as such is both efficient and practical.

The predictions were partially corroborated in direct measurements of the luminance tilts and chromatic axis rotations, although the empirical measurements did not reveal a significant effect for predicting the LvsM axis rotation. Also, we showed that the predictive capacity was marginally improved if the equiluminant settings along two axes were used in the prediction. As also noted, we only evaluated the simple linear correlations between the variables. In actual practice, the predictions could potentially be improved by incorporating the nonlinearities

in the relationships between the luminance and the chromatic angle changes as evident in Fig. 2 for the LvsM axis.

The discrepancies in the predictions for the LvsM axis were likely to result, in part, from the different criteria that the model and measurements used for defining this axis—and, specifically, whether the axis corresponded to constant *S*-cone activity (as in the adaptation protocol) or constant *S*-cone activity for lights of constant luminance (as in the model). These are equivalent for the standard observer, but our analyses show that they can depart for individual observers with different cone ratios so that the notion that the LvsM axis is synonymous with a constant-*S* axis is not generally valid. Barring a psychophysical procedure that can null the  $S/(L + M)$  signals (as opposed to *S* alone), our analyses suggest that the luminance variations may, in fact, provide a predictive estimate of the LvsM chromatic axis for observers with biased cone ratios, and a prediction which again is easily retrieved from psychophysical measurements that are already standard and easy to obtain.

**Funding.** National Institutes of Health (EY-010834).

**Disclosures.** The authors declare no conflicts of interest.

**Data availability.** Data underlying the results presented in this paper are not publicly available at this time but may be obtained from the authors upon reasonable request.

#### REFERENCES

1. B. B. Lee, "Color coding in the primate visual pathway: a historical view," *J. Opt. Soc. Am. A* **31**, A103–A112 (2014).
2. J. Krauskopf, D. R. Williams, and D. W. Heeley, "Cardinal directions of color space," *Vis. Res.* **22**, 1123–1131 (1982).
3. D. I. A. MacLeod and R. M. Boynton, "Chromaticity diagram showing cone excitation by stimuli of equal luminance," *J. Opt. Soc. Am.* **69**, 1183–1186 (1979).
4. A. M. Derrington, J. Krauskopf, and P. Lennie, "Chromatic mechanisms in lateral geniculate nucleus of macaque," *J. Physiol.* **357**, 241–265 (1984).
5. P. Lennie, J. Pokorny, and V. C. Smith, "Luminance," *J. Opt. Soc. Am. A* **10**, 1283–1293 (1993).
6. M. A. Webster and D. I. MacLeod, "Factors underlying individual differences in the color matches of normal observers," *J. Opt. Soc. Am. A* **5**, 1722–1735 (1988).
7. Y. Asano, M. D. Fairchild, and L. Blondé, "Individual colorimetric observer model," *PLoS ONE* **11**, e0145671 (2016).
8. K. A. G. Smet, M. A. Webster, and L. A. Whitehead, "Using smooth metamers to estimate color appearance metrics for diverse color-normal observers," *Color Res. Appl.* **47**, 555–564 (2022).
9. K. R. Lee, A. J. Richardson, E. Walowitz, M. A. Crognale, and M. A. Webster, "Predicting color matches from luminance matches," *J. Opt. Soc. Am. A* **37**, A35–A43 (2020).
10. O. N. Rood, "On a photometric method which is independent of color," *Am. J. Sci.* **3–46**, 173–176 (1893).
11. R. A. Bone and J. T. Landrum, "Heterochromatic flicker photometry," *Arch. Biochem. Biophys.* **430**, 137–142 (2004).
12. P. Cavanagh, D. I. MacLeod, and S. M. Anstis, "Equiluminance: spatial and temporal factors and the contribution of blue-sensitive cones," *J. Opt. Soc. Am. A* **4**, 1428–1438 (1987).
13. B. W. Tansley and R. M. Boynton, "A line, not a space, represents visual distinctness of borders formed by different colors," *Science* **191**, 954–957 (1976).
14. M. A. Webster, K. K. De Valois, and E. Switkes, "Orientation and spatial-frequency discrimination for luminance and chromatic gratings," *J. Opt. Soc. Am. A* **7**, 1034–1049 (1990).
15. M. A. Webster and J. D. Mollon, "The influence of contrast adaptation on color appearance," *Vis. Res.* **34**, 1993–2020 (1994).



16. M. A. Webster, E. Miyahara, G. Malkoc, and V. E. Raker, "Variations in normal color vision. I. Cone-opponent axes," *J. Opt. Soc. Am. A* **17**, 1535–1544 (2000).
17. V. C. Smith and J. Pokorny, "Chromatic-discrimination axes, CRT phosphor spectra, and individual variation in color vision," *J. Opt. Soc. Am. A* **12**, 27–35 (1995).
18. H. E. Smithson, P. Sumner, and J. D. Mollon, "How to find a Tritan line," in *Normal and Defective Colour Vision* (2003), pp. 279–287.
19. V. C. Smith, J. Pokorny, and S. J. Starr, "Variability of color mixture data—I. Interobserver variability in the unit coordinates," *Vis. Res.* **16**, 1087–1094 (1976).
20. M. A. Webster, E. Miyahara, G. Malkoc, and V. E. Raker, "Variations in normal color vision. II. Unique hues," *J. Opt. Soc. Am. A* **17**, 1545–1555 (2000).
21. J. Carroll, J. Neitz, and M. Neitz, "Estimates of L:M cone ratio from ERG flicker photometry and genetics," *J. Vis* **2**(8), 1 (2002).
22. A. Stockman, L. T. Sharpe, and C. Fach, "The spectral sensitivity of the human short-wavelength sensitive cones derived from thresholds and color matches," *Vis. Res.* **39**, 2901–2927 (1999).
23. L. T. Sharpe, A. Stockman, W. Jagla, and H. Jägle, "A luminous efficiency function,  $V^*(\lambda)$ , for daylight adaptation," *J. Vis* **5**(11), 948–958 (2005).
24. J. He, Y. Taveras-Cruz, and R. T. Eskew, Jr., "Modeling individual variations in equiluminance settings," *J. Vis* **21**(7), 15 (2021).